Immunol Res (2012) 52:240–249
DOI 10.1007/s12026-012-8332-4

Antitumor efficacy of viable tumor vaccine modified by heterogenetic ESAT-6 antigen and cytokine IL-21 in melanomatous mouse

Xiangfeng He · Jing Wang · Fengshu Zhao · Fangliu Yu · Dengyu Chen · Kai Cai · Cuiping Yang · Junsong Chen · Jun Dou

Published online: 5 April 2012

Abstract The goal of this study was to investigate whether glycosylphosphatidylinositol (GPI)-anchored 6 kDa early secreted antigenic target (ESAT-6) and IL-21-producing B16F10/ESAT-6-GPI-IL-21 viable vaccine would induce antitumor efficacy. Mice were immunized with B16F10/ESAT-6-GPI-IL-21 vaccine and challenged by B16F10 cells 2 weeks later. Antitumor efficacy and mechanisms of the vaccine were analyzed. Vaccination with the viable B16F10/ESAT-6-GPI-IL-21 vaccine resulted in an increase of IFN-γ level and the $CD8^+$CTL cytotoxicity, a decrease in TGF-β generation and increase in the expression of miR-200c that serves as melanoma suppressor by directly targeting zinc-finger E-box binding homeobox 1 to inhibit epithelial–mesenchymal transition and block tumor metastasis. The vaccine significantly inhibited the melanoma growth, reduced the lung melanoma nodules, and prolonged the mouse survival compared with the controls. These findings highlighted IL-21 as an immune adjuvant in an engineered viable tumor vaccine to reinforce heterogenetic antigen ESAT-6 immune tolerance break to induce powerful antitumor efficacy in mice.

Keywords Melanoma · Tumor vaccine · 6 kDa early secreted antigenic target · Interleukin-21 · Glycosylphosphatidylinositol

Introduction

Malignant melanoma is one of the deadliest forms of skin cancer and its incidence is expected to rise over the next two decades. At present, there are no effective therapies for advanced melanoma. Immunotherapeutic approaches for all kinds of cancers are currently emerging as promising strategies of antitumor therapy [1]. A growing body of literature shows that the vaccination is still a promising emerging treatment option. Using tumor cells as the primary immunogen provides a comprehensive source of tumor-associated antigens, thereby eliminating the need to identify individual antigens. Unfortunately, the malignant melanoma is a low immunogenic tumor incapable of stimulating potent antitumor immune responses. Tumor vaccines against melanoma require immune tolerance break since tumor-associated antigens used in vaccine formula are mostly self-antigens. If tumor cells are genetically engineered to express immune stimulatory cytokine, it is then a suitable approach to induce antitumor immune responses [2–4]. However, there exists a limitation in that tumor cells have developed numerous ways to escape immune surveillance and gain unlimited invasive and metastatic capacity. To overcome this limitation, a modified tumor vaccine with heterogenetic antigen tolerance break and cytokine potent activator can induce tumor-specific immunity [5].

The 6 kDa early secreted antigenic target (ESAT-6) is one the most immunodominant and highly *Mycobacterium tuberculosis*-specific antigen and contains multiple

Xiangfeng He, Jing Wang, and Fengshu Zhao equally contributed to this work.

X. He · F. Zhao · F. Yu · D. Chen · K. Cai · C. Yang · J. Chen · J. Dou (✉)
Department of Pathogenic Biology and Immunology, Medical School, Southeast University, Nanjing 210009, China
e-mail: njdoujun@yahoo.com.cn

J. Wang
Department of Gynecology and Obstetrics, Zhongda Hospital, Medical School, Southeast University, Nanjing 210009, China

immunogenic T/B cell epitopes and, therefore, is capable of enhancing immune responses. An ESAT-6 attribute is of primary importance in tuberculosis immunodiagnosis and vaccine development [6–8]. We therefore hypothesized that heterogenetic antigen ESAT-6 on the surface of tumor vaccine might be easily recognized by immune cells from melanoma-bearing mice and this would lead to tolerance break to elicit anti-melanoma immune response.

Glycosylphosphatidylinositol (GPI) is a post-translationally added lipid anchor, and GPI-anchored membrane cytokines have been shown to play an important role in host immune response against tumor cells [9–11]. Interleukin (IL)-21 is a T cell-derived cytokine that regulates an immune responses with the ability to regulate antitumor activity in mice and generates considerable research interest in understanding their mode of action [12–14]. The secreted IL-21 from the tumor vaccine or the application of low dose of IL-21 can exerts its antitumoral activity through the activation of the innate and acquired immune system. Therefore, IL-21 is being investigated in clinical phase I to II studies as a single drug on patients with metastatic melanoma [15–17].

We had previously shown that administering whole tumor cell vaccine expressing IL-21 in the GPI-anchored form induced protective anti-melanoma immunity in a B16F10 cell transplantable mouse model. However, the anti-melanoma efficacy was not completely satisfactory, highlighting the need for studying combination and alternative strategies [15]. To this end, we used a novel strategy for developing the viable tumor vaccine that was an ESAT-6-GPI and IL-21-producing B16F10 tumor vaccine (B16F10/ESAT-6-GPI-IL-21) to further investigate the immune effectiveness of anti-melanoma in the study. Furthermore, we evaluated possible mechanisms of this vaccine immune stimulation settings relevant to melanoma.

Materials and methods

Mice, cells, and primes

C57BL/6 mice of 6–8 week of age were obtained from the Yangzhou University of China. All mice were housed under the pathogen-free condition, and the experiments were performed in compliance with the guidelines of the Animal Research Ethics Board of Southeast University. Full details of the study approval can be found in the approval ID: 20080925. The B16F10 murine melanoma cell line is syngeneic in C57BL/6 mice, and YAC-1 cell line is Moloney leukemia-induced T cell lymphoma of A/Sn mouse origin, obtained from the Cellular Institute of China in Shanghai. These cells were cultured at 37 °C in 5 % CO_2 atmosphere in RPMI 1640 supplemented with 10 % fetal bovine serum that contained 100 U ml^{-1} penicillin G sodium and 100 mg ml^{-1} streptomycin sulfate.

The sequences of the primers are as follows:

miR 200c: RT Primer, 5′-GTCGTATCCAGTGCA GGGTCCGAGGTATTCGCACT GGATACGACTCCAT CAT-3′; sense, 5′-GCCCGCTAATACTGCCGGGTA-3′; U6: RT Primer, 5′-GTCGTATCCAG TGCAGGGTCCGA GGTATTCGCACTGGATACG ACAAATATGGAAC-3′; sense, 5′-TGCGGGTGCTCGCTTCGGCAGC-3′; URP (Universal Reverse Primer), 5′-CCAGTGCAGGGTCCG AGGT-3′. All the primers were synthesized by Company of Gene and Technology of China in Shanghai.

Development of B16F10 tumor vaccine expressing ESAT-6-gpi and IL-21

The construction of pRSC-ESAT-6-GPI-IL-21 was done in the same way as in our previous reports [3, 15]. As a control, the pRSC-IL-21 and pRSC-ESAT-6-GPI were, respectively, generated as well. The different recombinants were separately transfected into the B16F10 cells using Lipofectamine™ 2000 reagent (Invitrogen, USA) according to the manufacturer's protocol. The stably expressing ESAT-6-GPI and IL-21 cells, the ESAT-6-GPI cells, and the IL-21 cells were, respectively, selected from RPMI containing 800 mg/ml G418 (Clontech, CA) and cloning by limiting dilution. We named B16F10/ESAT-6-GPI-IL-21 cells for the cells expressing GPI-ESAT-6 and IL-21, B16F10/ESAT-6-GPI cells for the cells expressing ESAT-6-GPI, B16F10/IL-21 cells for the cells expressing IL-21 cells, and B16F10/mock cells for the cells with no expression.

Detection of expressions of ESAT-6-GPI and IL-21 in B16F10/ESAT-6-GPI-IL-21 cells and analysis of expressions of TGF-β1, N-cadherin, and E-cadherin in the tumor tissues

Expression of ESAT-6-GPI was detected by an immunofluorescence assay in the same way as in our previous report [3]. Briefly, the different cells were fixed with 4 % paraform for 10 min and were blocked with Tris-buffered saline with Tween containing 5 % bovine serum albumin at 37 °C for 40 min and then incubated with rat anti-ESAT-6 at 4 °C overnight, rinsed three times in PBS, and then the cells were incubated with rabbit anti-rat IgG labeled with phycoerythrin (eBioscience company, USA) at 37 °C for 1 h. Finally, the cells on the glass were observed by the fluorescence microscope. Western blot was used to analyze the expressions of IL-21, transforming growth factor-β (TGF-β), mesenchymal protein (N-cadherin), and epithelial protein (E-cadherin) in the vaccinated tumor tissues. Briefly, 1×10^6 cells were collected and lyzed in a protein

extraction buffer (Novagen, WI, USA) according to the manufacturer's protocol. 12 % sodium dodecyl sulfate–polyacrylamide gel electrophoresis and 15 μg proteins/lane were electrotransferred onto a nitrocellulose membrane. The goat anti-mouse IL-21 (I-18, Santa Cruz Biotechnology Company) or goat anti-mouse TGF-β1 (Biowold Company) or goat anti-mouse E-cadherin (R868, Biowold Company) or goat anti-mouse N-cadherin (w745, Biowold Company) was, respectively, added to the membrane for 1 h, and the membrane was washed for 5 min with antibody wash solution three times, and the subsequent steps were performed according to the Western Blot Kit's protocol (Pierce Company) [18].

Animal experiments

In the safe experiment of tumor vaccines, C57BL/6 mice were randomly divided into B16F10/mock cell group, B16F10/IL-21 cell group, B16F10/ESAT-6-GPI cell group, and B16F10/ESAT-6-GPI-IL-21 cell group. Each mouse was immunized subcutaneous (s.c.) with 2×10^5 different cells described above, respectively, to observe the oncogenicity of the tumor vaccines.

Three antitumor experiments were carried out. In the first experiment, C57BL/6 mice were randomly divided into the four groups as described above. Each mouse was immunized s.c. in the flanks with 2×10^5 different tumor cell vaccine and 2 weeks after the immunization, 1×10^5 B16F10 cells were challenged into the abdominal part of each mouse. In the second experiment, C57BL/6 mice were divided into three groups. The first group mice were inoculated s.c. in the right abdominal area with 1×10^5 B16F10/mock cells. The second group mice were immunized with the 2×10^5 B16F10/ESAT-6-GPI-IL-21 vaccine in the left abdominal area and were simultaneously challenged with the 1×10^5 B16F10 cells in the right abdominal area. The third group mice were inoculated s.c. in the right abdominal area with both 1×10^5 B16F10 cells and 2×10^5 B16F10/ESAT-6-GPI-IL-21 vaccine. Tumor growth was observed for 60 days. The tumors were felt by touch in the mice, and tumor growth was monitored twice a week by measuring two perpendicular tumor diameters using calipers, and then the tumor volume, tumor-free mice %, and survival mice were evaluated, respectively. In the third experiment, C57BL/6 mice were divided into a prophylactic melanoma group and a control group. 2×10^5 B16F10 cells were injected into each mouse by its lateral tail vein on 14 days after 2×10^5 B16F10/ESAT-6-GPI-IL-21 vaccine or 2×10^5 B16F10/mock cell vaccine were, respectively, immunized s.c. in the mouse's right flank. Twenty days after the lateral tail vein injection, the mice were killed for detecting the melanoma nodule numbers in the lungs.

Assays of splenocyte proliferative response, ratio of $CD4^+/CD8^+$ T lymphocytes, and cytotoxicities of CTL and NK cells

Two weeks after the final immunization, 5×10^6 splenocytes were prepared from the C57BL/6 mice immunized with the 2×10^5 B16F10/ESAT-6-GPI-IL-21 vaccine or the 2×10^5 B16F10/mock cell vaccine. The harvested splenocytes were labeled with 0.5 mM 5-(and 6)-carboxyfluorescein diacetate succinimidyl ester (CFSE; 20 μg/ml) at 37 °C for 15 min. The splenocytes were washed twice in PBS containing 5 % fetal bovine serum to sequester any free CFSE. 2×10^6 splenocytes were resuspended in an 10 % RPMI medium in 24-well plates and then incubated for 72 h with the supernatant from the cultured B16F10/ESAT-6-GPI-IL-21 or B16F10/IL-21 or B16F10/mock cells in the proliferative assay [18, 19]. $CD8^+$ lymphocytes were isolated by magnetic column selection or depletion (MACS, Miltenyi Biotec) [20, 21]. In $CD8^+$ cytotoxic T lymphocytes (CTL) and NK cytotoxic assays, the B16F10 cells and YAC-1 cells were, respectively, used as target cells, $CD8^+$ lymphocytes and splenocytes were used as effector cells. All cytotoxicity assays were performed in triplicate. Flow cytometric CFSE/7-AAD cytotoxicity assays were analyzed by Flow Cytometry (FCM, BD company, USA) [15, 22]. In assay for the ratio of $CD4^+/CD8^+$ T lymphocytes, the cells were from the splenocytes and the groin lymph nodes in the immunized mice and the lymphocyte phenotypes were detected by FCM [3].

ELISA for IFN-γ and anti-ESAT-6

The serum IFN-γ level and anti-ESAT-6 serum were measured using a commercially available enzyme linked-immunosorbent assay (ELISA) according to the manufacturer's protocol (eBioscience) [23, 24].

Complement-dependent cytotoxicity (CDC) and detection of apoptotic tumor cells phagocytized by dendritic cells (DCs)

For the determination of CDC, 2×10^5 B16F10/ESAT-6-GPI-IL-21 cells were plated into a 96-well plate and the immunized mouse serum that include anti-ESAT-6 and complement was added to the wells at different concentrations. Cells were incubated for 4 h, and the resulting absorption was analyzed at 490 nm using a spectrophotometer. CDC was calculated according to the Ref. [25]. To prepare autologous DCs from mouse bone marrow, the protocol was performed as described previously [26]. The collected DCs were, respectively, used for incubation together with the DiI-labeled B16F10/ESAT-6-GPI-IL-21 cells or B16F10/mock cells and the immunized mouse

serum. After 12 h incubation and washing, the precipitated cells were stained with FITC-conjugated anti-CD11c (eBioscience, USA). Apoptotic tumor cells (red) phagocytized by DCs (green) were analyzed using immunofluorescence microscope, and the phagocytosis efficacy was detected using flow cytometry [27].

Quantitative reverse transcriptase-PCR (qRT-PCR)

Total cellular RNA was extracted from the tumor tissue cells by using RNeasy Mini Kit (Qiagen, CA) according to the manufacture's instructions. cDNA was synthesized with the reverse SuperScript Choice System (Invitrogen, CA). TaqMans MicroRNA Assays for miR-200c and control U6 were carried out for each sample (an ABI 7300 real-time system, PE Applied Biosys tems) [28, 29].

Statistical analysis

The Student's t test or Log-rank test or Paired t test was used to calculate differences between the different experimental conditions. The Bonferroni correction for multiple comparisons was used to determine significant differences. Differences were regarded significant if $p < 0.05$.

Results

Detecting target protein expressions in the engineered B16F10 tumor vaccine and its bioactivities

To generate tumor cells secreting the IL-21 and GPI-anchored membrane ESAT-6, we constructed the B16F10/ESAT-6-GPI-IL-21 cells. Figure 1a, b reflects that IL-21 was correctly expressed in the B16F10/IL-21 cells and the B16F10/ESAT-6-GPI-IL-21 cells, and that ESAT-6 was actually anchored on the surface of B16F10/ESAT-6-GPI or on the B16F10/ESAT-6-GPI-IL-21 cells via GPI, but not on the surface of the B16F10/mock cells.

Furthermore, we identified the IL-21 and a ESAT-6 bioactivities of the B16F10/ESAT-6-GPI-IL-21 or the B16F10/IL-21 or the B16F10/ESAT-6-GPI cells, respectively. The splenocyte's proliferative activities in the different groups were statistically significant for both the B16F10/ESAT-6-GPI-IL-21 cell group and the B16F10/IL-21 cell group in comparison with the B16F10/mock cell group ($p < 0.005$ or $p < 0.01$, Fig. 1c). The ESAT-6-GPI bioactivity was identified with the detection of anti-ESAT-6 in the immunized mice (Fig. 1d). The serum antibody level in mice immunized with the B16F10/ESAT-6-GPI cells or the B16F10/ESAT-6-GPI-IL-21 cells was significantly increased ($p < 0.005$) compared with the level in mice immunized with the B16F10/mock cells (Fig. 1e). These results suggested that the IL-21 secreted from the B16F10/ESAT-6-GPI-IL-21 or the B16F10/IL-21 cells as well as the ESAT-6 on the B16F10/ESAT-6-GPI or on the B16F10/ESAT-6-GPI-IL-21 cells were functional, and that these cells would provide an effective tumor cell vaccine for further therapy of melanoma in the mouse model.

Evaluation of tumor vaccine anti-melanoma efficacy

In the safe experiment of tumor vaccines, there were tumor generation in 10/10 mice inoculated with the 1×10^5 B16F10/mock cells or 8/10 mice inoculated with the 1×10^5 B16F10/ESAT-6-GPI cells or in 4/10 inoculated with the 1×10^5 B16F10/IL-21 cells in 30 days. No tumor generation was, however, found in the 10 mice inoculated with 1×10^5 B16F10/ESAT-6-GPI-IL-21 cells in 60 days (Fig. 2a). Moreover, no tumor generation was observed in another 12 mice inoculated with the 2×10^5 viable B16F10/ESAT-6-GPI-IL-21 cells until 60 days into the observation (data no shown). Consequently, the 2×10^5 viable B16F10/ESAT-6-GPI-IL-21 cells as tumor vaccine without any treatment were considered safe and effective. Subsequently, they were used to investigate anti-tumor efficacy.

Figure 2b indicates that two of the 14 mice immunized with the 2×10^5 B16F10/ESAT-6-GPI-IL-21 vaccine developed tumors on Day 28 and Day 35 and that 7 of the 14 mice immunized with the 2×10^5 B16F10/IL-21 vaccine formed tumors on Day 20, Day 26, Day 28, Day 32, Day 34, and Day 35, and that nine of the 14 mice immunized with 2×10^5 B16F10/ESAT-6-GPI vaccine formed tumors in 35 days after 1×10^5 B16F10 cells challenged in the different vaccine groups, respectively. In contrast, after the 1×10^5 B16F10 cells challenged, all the 14 mice immunized with the 2×10^5 B16F10/mock cell vaccine formed tumors in Day 28. Figure 2e1–e3 shows three kinds of different experiments in order. In the prophylactic lung melanoma experiment, it was found that the tumor nodules were obviously reduced in numbers in the mice immunized with B16F10/ESAT-6-GPI-IL-21 vaccine when compared with the mice immunized with an inactivated B16F10/mock cell vaccine. It is thus evident that the anti-melanoma efficacy of the B16F10/ESAT-6-GPI-IL-21 vaccine was well demonstrated through these experiment results.

Analysis of ratio of $CD4^+/CD8^+$ T lymphocytes and cytotoxicities of CTL and NK cells in the immunized mice

Since the B16F10/ESAT-6-GPI-IL-21 vaccine has stronger anti-melanoma efficacy than other vaccines (Fig. 2b), we wanted to explore the mechanisms of this anti-melanoma efficacy induced by the B16F10/ESAT-6-GPI-IL-21

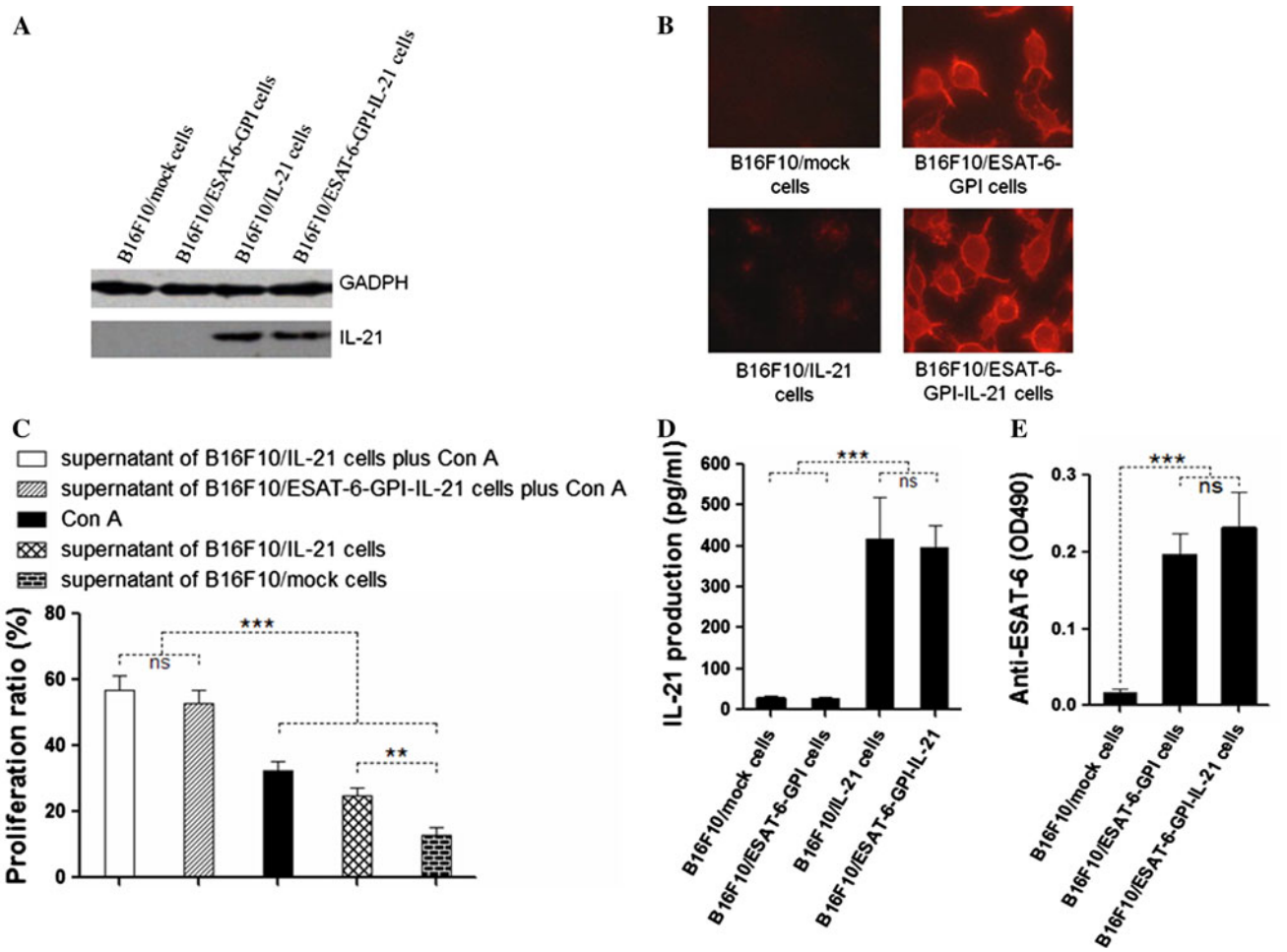

Fig. 1 Target protein expressions and its bioactivities. IL-21 expression was detected by Western blot as shown in **a**. IL-21 was correctly expressed in the B16F10/IL-21 cells and the B16F10/ESAT-6-GPI-IL-21 cells. An expression of ESAT-6-GPI was measured by immunofluorescence assay. **b** Exhibits that ESAT-6 was actually anchored on the surface of B16F10/ESAT-6-GPI or on the B16F10/ESAT-6-GPI-IL-21 cells via GPI, but not on the surface of the B16F10/mock cells. The splenocyte's proliferative activities in the different groups were detected by MTT assay as shown in **c**. The amount of IL-21 secreted by the cultured cells was measured by ELISA as shown in **d**. An ESAT-6-GPI bioactivity was identified with the detection of anti-ESAT-6 in the mice immunized with the B16F10/ESAT-6-GPI cells or the B16F10/ESAT-6-GPI-IL-21 cells two times at 14-day apart as shown in **e**. $***p < 0.005$, $**p < 0.01$

vaccine compared with the B16F10 vaccine alone in our subsequent study. The results given in Fig. 3a indicate that the ratios of $CD4^+/CD8^+$ T lymphocytes were lower in the splenocytes and the groin lymph nodes of mice immunized with the B16F10/ESAT-6-GPI-IL-21 vaccine than that of mice immunized with the B16F10/mock vaccine. The data suggest that $CD8^+$ phenotype T lymphocytes were significantly increased in the splenocytes and the groin lymph nodes after the B16F10/ESAT-6-GPI-IL-21 vaccine were immunized. Figure 3b further confirmed that the activity of $CD8^+$ CTL was increased in mice immunized with the B16F10/ESAT-6-GPI-IL-21 vaccine compared with the mice immunized with the B16F10/mock vaccine.

The NK cytotoxicity to the YAC-1 cells indicated that the higher cytotoxicity was in the mice immunized with the B16F10/ESAT-6-GPI-IL-21 cells (48.21 %) than that of the mice immunized with the B16F10/mock cells (21.16 %) as is shown in Fig. 3b. These results implied that the heterogenetic antigen ESAT-6 may mediate naive T lymphocytes to differentiate into effector $CD8^+$ T lymphocytes; meanwhile, immune adjuvant IL-21 may augment the cytotoxicities of $CD8^+$CTL and NK cells to the B16F10 cells, or YAC-1 cells, respectively.

Serum IFN-γ, CDC, and phagocytosis of DCs

Having found that the cytotoxicities of CTL and NK cells were significantly increased in the mice vaccinated with the B16F10/ESAT-6-GPI-IL-21 vaccine, we wanted to determine whether this effect also had an impact on the serum IFN-γ level and the activity of CDC as well as phagocytosis of DCs. Figure 4a shows that the serum IFN-γ level was significantly increased in the B16F10/ESAT-6-GPI-IL-21 vaccine group compared with the B16F10/mock

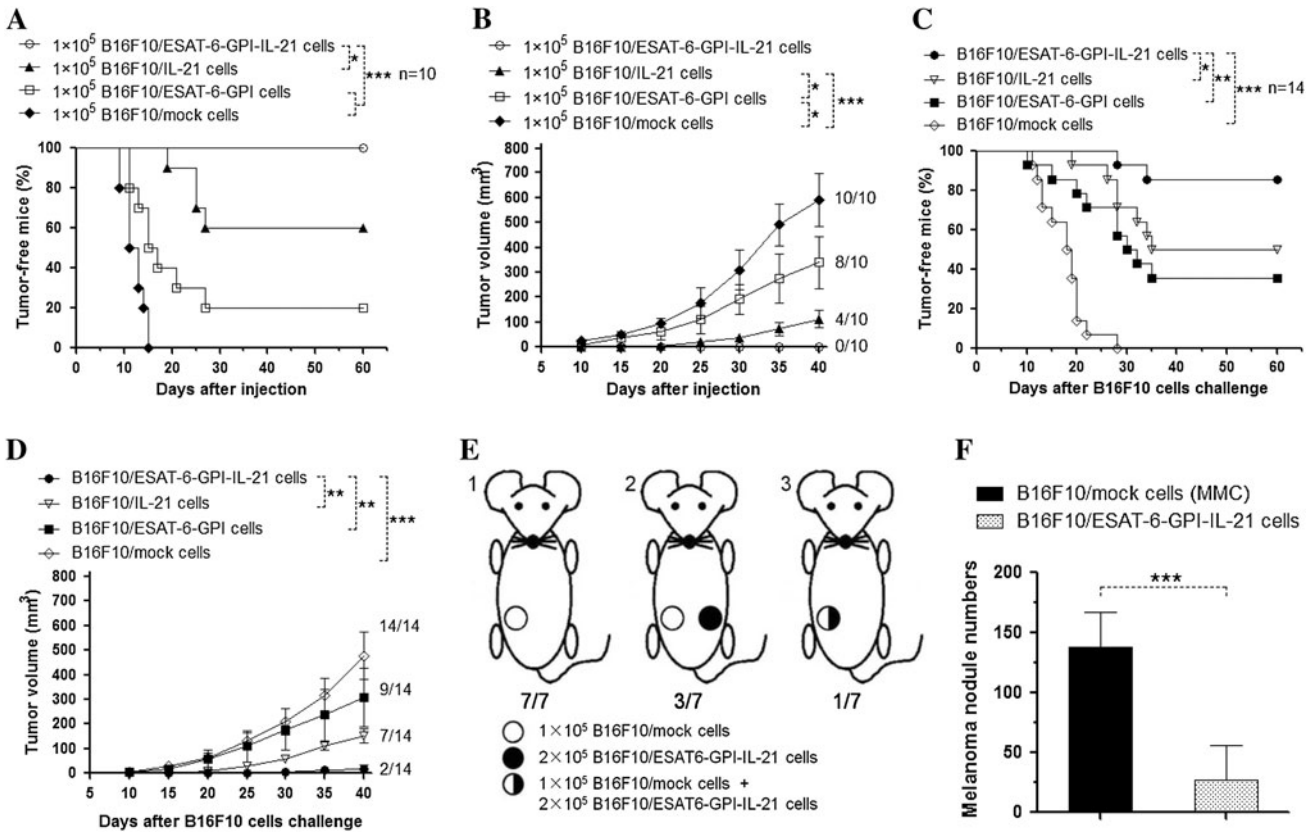

Fig. 2 Anti-melanoma efficacy induced by the different tumor cell vaccines. **a** Shows the oncogenicity in mice s.c. challenged with 1×10^5 different tumor vaccines. **b** Indicates the tumor volume of mice after the different tumor vaccine injection. **c** Indicates the antitumor experiment results in where the mice were vaccinated with 2×10^5 different tumor vaccines and were then s.c. challenged with 1×10^5 B16F10 cells after 2 weeks and the tumor volume was shown in **d**. **e**1 shows that 7 of the 7 mice immunized with the 1×10^5 B16F10/mock cells developed tumors in the inoculated right site in 25 days. **e**2 shows that 3 of the 7 mice developed tumors challenged with 1×10^5 B16F10 cells in the right site and immunized with 2×10^5 B16F10/ESAT-6-GPI-IL-21 cells in the left site simultaneously. **e**3 shows that 1 of the 7 mice developed tumor in 48 days after the mice were immunized with the 2×10^5 B16F10/ESAT-6-GPI-IL-21 cells mixed with 1×10^5 B16F10 cells. Three kinds of different *color circles* in **e** represent the inoculated various cells. **f** Shows the lung melanoma nodule numbers in mice immunized with B16F10/mock cells and B16F10-ESAT-6-gpi/IL-21 cells. Log-rank test was used in **a** and **d**. Student's *t* test was used in **f**. Significant differences are indicated by asterisk for $*p < 0.05$, $**p < 0.01$, and $***p < 0.005$

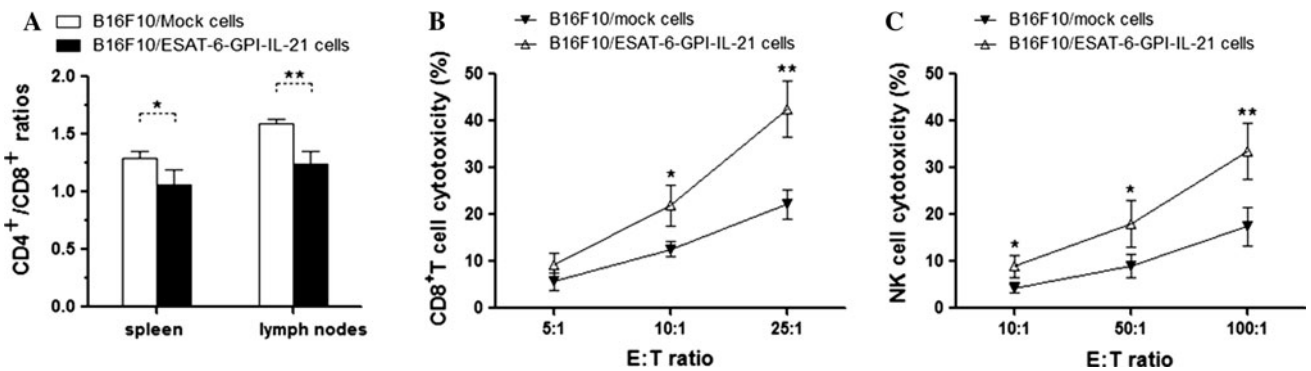

Fig. 3 Ratio of $CD4^+/CD8^+$ T lymphocytes and cytotoxicities of CTL and NK analyzed by FCM. **a** Shows the ratios of $CD4^+$T cells/$CD8^+$T cells in the splenocytes and the groin lymph nodes of mice immunized with the B16F10/ESAT-6-GPI-IL-21 vaccine and the B16F10/mock vaccine. The cytotoxicities of $CD8^+$T cells and NK cells in mice immunized with the B16F10/ESAT-6-GPI-IL-21 vaccine were detected by FCM as shown in **b**, **c**. A representative set of data for seven mice was used and an experiment repeated twice. Significant differences are indicated by *asterisk* for $*p < 0.05$ and $**p < 0.01$

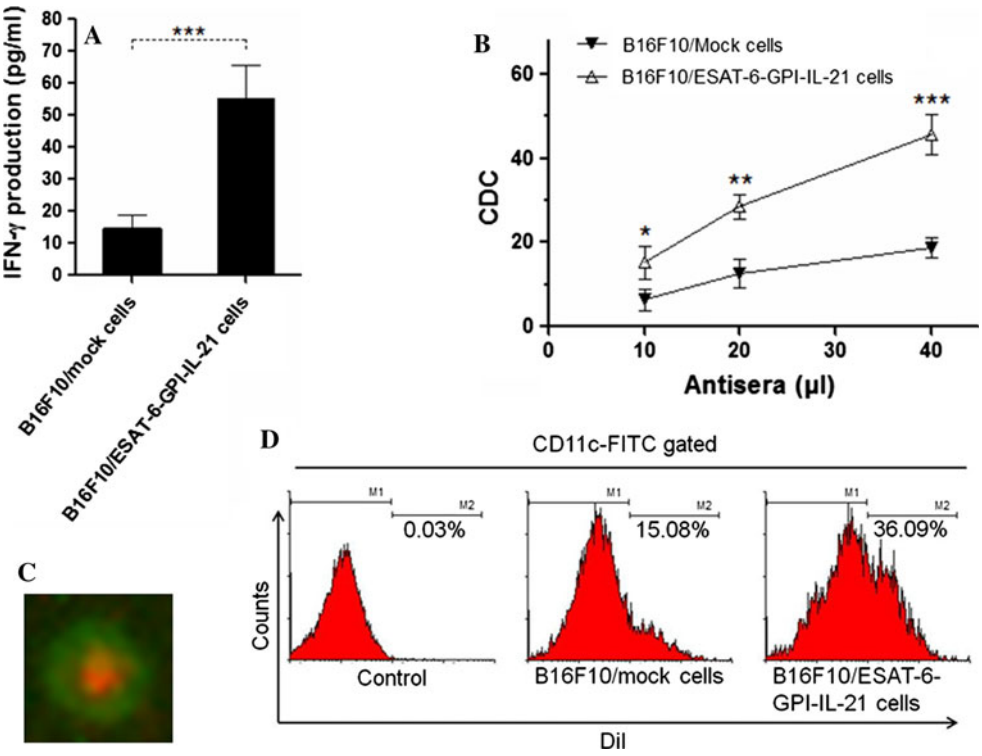

Fig. 4 Detection of serum IFN-γ level, CDC activity, and phagocytosis of DCs. **a** Shows the serum IFN-γ level detected by ELISA. CDC activity was detected by complement-dependent cytotoxicity assay using B16F10/ESAT-6-GPI-IL-21 cells and immunized mouse serum as shown in **b**. The data shown are for the seven mice and the experiments were repeated twice. **c** Indicates the image of apoptotic tumor cell (*red*) phagocytized by purified DC (*green*) detected by immunofluorescence microscope. The phagocytosis percent of DCs in the different groups is shown in **d**. Significant differences are indicated by *asterisk* for $*p < 0.05$, $**p < 0.01$, and $***p < 0.005$ (Color figure online)

vaccine group ($p < 0.005$). Figure 4b indicates that the higher activity of CDC was found in the mice vaccinated with the B16F10/ESAT-6-GPI-IL-21 vaccine than in the mice vaccinated the B16F10/mock vaccine. The result suggested that B16F10/ESAT-6-GPI-IL-21 tumor cell vaccine could be killed by the CDC. The lytic cells contain some apoptotic B16F10/ESAT-6-GPI-IL-21 cells (red) that were phagocytized by DCs (green) as is shown in Fig. 4c. The phagocytosis percent was significantly increased in the B16F10/ESAT-6-GPI-IL-21 cells (39.06 %) compared with the B16F10/mock cells (15.08 %, $p < 0.01$) as is shown in Fig. 4d.

Evaluation of molecular markers of EMT and detection of TGF-β and miR-200c expressions

There has been evidence that aberrant activation of the embryonic program epithelial–mesenchymal transition (EMT) promotes tumor cell invasion and metastasis [30]. The loss of an epithelial phenotype and the acquisition of mesenchymal characteristics are the key steps in a manner highly reminiscent of EMT [31]. Could it be that the melanoma in the mouse model is associated with EMT? To this end, we detected the characteristic biomarkers of E-cadherin (epithelial cells) and N-cadherin (mesenchymal cells) [32]. Figure 5a shows that the E-cadherin expression was markedly increased, but the N-cadherin expression was dramatically downregulated in the melanoma tissues in the mice vaccinated with the B16F10/ESAT-6-GPI-IL-21 vaccine compared with the mice vaccinated with the B16F10/mock vaccine. What may have caused the change to these characteristic proteins of EMT? A recent study addressed EMT in melanoma upon expression of TGF-β that increased zinc-finger E-box binding homeobox 1 (ZEB1) level but the miRNA 200c inhibited ZEB1 and increased the expression of ZEB1-repressed epithelial genes such as E-cadherin [33, 34]. Therefore, we further detected the expressions of TGF-β1, ZEB1, and miR-200c in tumor tissues. In Fig. 5a, b, the expressions of TGF-β1and ZEB1 were decreased, but miR-200c was upregulated in the B16F10/ESAT-6-GPI-IL-21 vaccine-immunized mice compared with the B16F10/mock vaccine-immunized mice (Fig. 5c). This finding was of significance.

Discussion

We engineered viable B16F10/ESAT-6-GPI-IL-21 tumor vaccine, in which an ESAT-6 acts as heterogenetic antigen on the membrane surface of B16F10 cells and IL-21 acts as a promising immune adjuvant, that could break melanoma immune tolerance and enhance the vaccine's effect of anti-melanoma immune tolerance in the tumor-bearing mice, which was reflected in the protection against melanoma challenge (Fig. 2b), in the suppression of melanomatous growth (Fig. 2c) and in the decrease in melanoma nodule numbers in the murine lung (Fig. 2d). Clearly, this

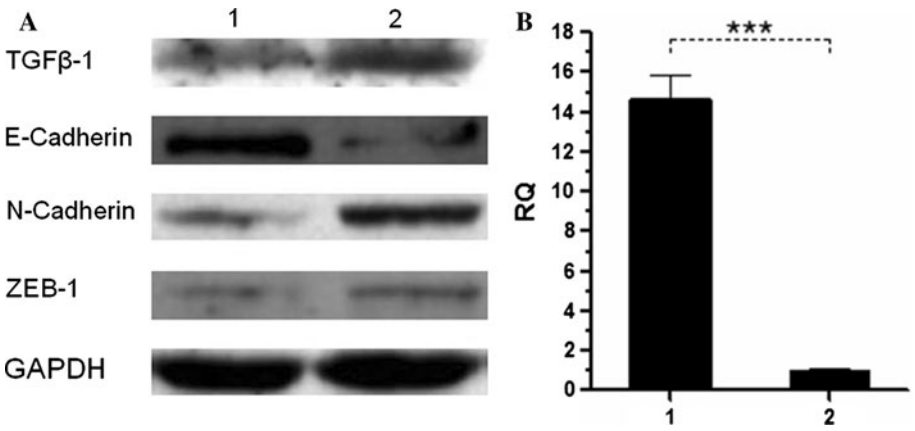

Fig. 5 EMT phenotype identification and expressions of TGF-β and miR-200c. **a** Shows that the results of Western blot. The samples were taken from the tumor tissues in the mice immunized with the B16F10/ESAT-6-GPI-IL-21 vaccine (*line 1*) and the B16F10/mock cells (*line 2*). The miR-200c expression detected by qRT-PCR was significantly increased (***$p < 0.005$) in the B16F10/ESAT-6-GPI-IL-21 cells (*line 1*) in contrast to the B16F10/mock cells (*line 2*) in **b**

antitumoral effect signifies that this new vaccine not only has an advantage over the B16F10/mock vaccine used for the control, but also is better than our previous developed B16F10/IL-21-GPI tumor vaccine [15] or B16F10/IL-21-GPI-GM-CSF tumor vaccine [3]. Those two vaccines that we previously developed were inactivated by mitomycin C (100 μg/ml) and required three immunizations at 14-day intervals. Our newly developed B16F10/ESAT-6-GPI-IL-21 vaccine in this study is a viable tumor vaccine and needs only one immunization to induce strong anti-melanoma effect. Figure 2b indicates that only two of the 14 mice vaccinated with B16F10/ESAT-6-GPI-IL-21 vaccine developed tumors that had delayed generation, were small, stayed at their original volume after 40 days, and did not grow larger. One of two tumors actually became gradually smaller than it was 40 days ago, but it did not disappear. However, our engineered other vaccine did not generate as strong antitumor immunity as the viable B16F10/ESAT-6-GPI-IL-21 vaccine did.

Regarding the tumor vaccine efficacy in the mice, we believe that the anti-melanoma role depended mainly on the mice's immune responses. The B16F10/ESAT-6-GPI-IL-21 vaccine firstly elicited anti-ESAT-6 generation and further activated complement classical pathway after anti-ESAT-6 bound ESAT-6 on the surface of B16F10/ESAT-6-GPI-IL-21 cells to form immune complex that resulted in CDC and killed the B16F10/ESAT-6-GPI-IL-21 cells. The lytic cells may contain some apoptotic B16F10/ESAT-6-GPI-IL-21 cells and tumor antigens, which served as a potential potent trigger for the initiation of tumor immunity. This was revealed by the increased $CD^{+}8$ T cell phenotype, the enhanced cytotoxicities of NK cells and $CD8^{+}$CTL, and the elevated serum IFN-γ level in the vaccinated mice. Although heterogenetic antigen ESAT-6 broke immune tolerance to stimulate strong immune responses in the mouse melanoma model and IL-21 acted as a tumor vaccine adjuvant to improve murine antitumor efficacy, the data suggest that neither the B16F10/ESAT-6-GPI vaccine nor the B16F10/IL-21 vaccine generated as stronger anti-melanoma efficacy as the B16F10/ESAT-6-GPI-IL-21 vaccine did. The reasons may be that the single-handed vaccine efficacy, the B16F10/ESAT-6-GPI, or the B16F10/IL-21 was limited against melanoma in current study.

It is now evident that the model of a feedback loop links ZEB1 to miR-200c, and that ZEB1 and miR-200c repress each other in the loop. In tumors, environmental TGFβ1 could trigger an upregulation of ZEB1, promoting a self-enhancing loop in tumor cells, and resulting in EMT and invasion [32, 34, 35]. Figure 5a indicates that TGFβ1 and ZEB1 were downregulated in the tumor tissues of mice vaccinated with the B16F10/ESAT-6-GPI-IL-21 vaccine compared with the mice vaccinated with the B16F10/mock vaccine, also consistent with TGFβ1 and ZEB1 being involved in the process of EMT [31]. miR-200c was upregulated in the tumor tissues of mice vaccinated with the B16F10/ESAT-6-GPI-IL-21 vaccine. Depending on the decrease in the initial signal TGFβ1, we hypothesize an immune response induced by the B16F10/ESAT-6-GPI-IL-21 vaccine might influence the aforementioned feedback loop that may stabilize epithelial differentiation and block EMT in the mice. Given that a metastatic melanoma is one of the main causes for high mortality in human malignant melanoma. An effective vaccine should be capable of maximizing the effect of prevented melanoma metastases. We have developed the B16F10/ESAT-6-GPI-IL-21 vaccine to inhibit TGFβ1 generation and to promote the expression of miR-200c, which acts as a tumor suppressor

by directly targeting ZEB1 to limit EMT and prevent melanoma metastases that were markedly reduced in tumor nodule numbers in the mouse lungs (Fig. 2d). Nevertheless, we still are uncertain about an expressive changes of miR-200c and ZEB1 in an exactly cells since these molecular detections were based on the tumor tissue samples. As all know, the tumor tissues in the vaccinated mice included the B16F10 cells, the B16F10/ESAT-6-GPI-IL-21 cells, or the B16F10/mock cells; an extracellular matrix; tumor-associated fibroblasts; bone marrow-derived cells; and tumor epithelial cells [36]. Further task, therefore, needs to do in order to find which cells made a key function in these molecule expressive changes.

Taken together, in this mouse tumor model, vaccination with the viable B16F10/ESAT-6-GPI-IL-21 tumor cell vaccine induced powerful antitumor responses to autologous tumors by eliciting cellular and humoral immunologic responses, inhibiting TGFβ1 generation, and promoting expression of miR-200c. Our findings suggest that the ESAT-6-GPI can be a novel heterogenetic antigen anchored in producing immune adjuvant IL-21 tumor cell vaccine with the effective antitumor immunity for melanoma immunotherapy. The regimen may be a promising therapeutic agent against melanoma.

Acknowledgments This work was partly supported by the National Natural Science Foundation of China (No. 81071769).

Conflict of interest The authors have no conflicting financial interests.

References

1. Tanaka A, Jensen JD, Prado R, Riemann H, Shellman YG, Norris DA. Whole recombinant yeast vaccine induces antitumor immunity and improves survival in a genetically engineered mouse model of melanoma. Gene Ther. 2011;18:827–34.
2. Asemissen AM, Brossart P. Vaccination strategies in patients with renal cell carcinoma. Cancer Immunol Immunother. 2009; 58:1169–74.
3. Fengshu Z, Jun D, Xiangfeng H, Chu LL, Hu WH, Yu FL. Enhancing therapy of B16F10 melanoma efficacy through tumor vaccine expressing GPI-anchored IL-21 and secreting GM-CSF in mouse model. Vaccine. 2010;28:2846–52.
4. Triozzi PL, Aldrich W, Achberger S, Ponnazhagan S, Alcazar O, Saunthararajah Y. Differential effects of low-dose decitabine on immune effector and suppressor responses in melanoma-bearing mice. Cancer Immunol Immunother. 2012; Feb 5 [Epub ahead of print].
5. Restifo NP. Building better vaccines: how apoptotic cell death can induce inflammation and activate innate and adaptive immunity. Curr Opin Immunol. 2000;12:597–603.
6. Millington KA, Fortune SM, Low J, Garces A, Hingley-Wilson SM, Wickremasinghe M, Kon OM, Lalvani A. Rv3615c is a highly immunodominant RD1 (Region of Difference 1)-dependent secreted antigen specific for *Mycobacterium tuberculosis* infection. Proc Natl Acad Sci USA. 2011;108:5730–5.
7. Olsen AW, Hansen PR, Holm A, Andersen P. Efficient protection against *Mycobacterium tuberculosis* by vaccination with a single subdominant epitope from the ESAT-6 antigen. Eur J Immunol. 2000;30:1724–32.
8. Ganguly N, Giang PH, Basu SK, Mir FA, Siddiqui I, Sharma P. *Mycobacterium tuberculosis* 6-kDa early secreted antigenic target (ESAT-6) protein downregulates lipopolysaccharide induced c-myc expression by modulating the extracellular signal regulated kinases 1/2. BMC Immunol. 2007;8:24.
9. Ji JF, Li JH, Lillia MH. Synergistic anti-tumor effect of glycosylphosphatidylinositol-anchored IL-2 and IL-12. J Gene Med. 2004;6:777–85.
10. Naghibalhossaini F, Yoder AD, Tobi M, Stanners CP. Evolution of a tumorigenic property conferred by glycophosphatidyl-inositol membrane anchors of carcinoembryonic antigen gene family members during the primate radiation. Mol Biol Cell. 2007;18: 1366–74.
11. Butikofer P, Malherbe T, Boschung M. GPI-anchored proteins: now you see 'em, now you don't'. FASEB J. 2001;15:545–8.
12. Parrish-Novak J, Dillon SR, Nelson A, Hammond A, Sprecher C, Gross JA. Interleukin and its receptor are involved in NK cell expansion and regulation of lymphocyte function. Nature. 2000;408:57–63.
13. Davis ID, Skak K, Smyth MJ, Kristjansen PE, Miller DM, Sivakumar PV. Interleukin-21 signaling: functions in cancer and autoimmunity. Clin Cancer Res. 2007;13:6926–32.
14. Smyth MJ, Teng MW, Sharkey J, Wertwood JA, Haynes NM, Yagita H. Interleukin 21 enhances antibody-mediated tumor rejection. Cancer Res. 2008;68:3019–25.
15. Fengshu Z, Jun D, Jing W, Xiangfeng H, Hu WH. Investigation on the anti-tumor efficacy by expression of GPI-anchored mIL-21 on the surface of B16F10 cells in C57BL/6 mice. Immunobiology. 2010;215:89–100.
16. Thompson JA, Curti BD, Redman BG. Phase I study of recombinant interleukin-21 in patients with metastatic melanoma and renal cell carcinoma. J Clin Oncol. 2008;26:2034–9.
17. Frederiksen KS, Lundsgaard D, Freeman JA. IL-21 induces in vivo immune activation of NK cells and CD8(1) T cells in patients with metastatic melanoma and renal cell carcinoma. Cancer Immunol Immunother. 2008;57:1439–49.
18. Weihua H, Jing W, Jun D. Augmenting therapy of ovarian cancer efficacy by secreting IL-21 human umbilical cord blood stem cells in nude mice. Cell Transplant. 2011;20:669–80.
19. Jun D, Guobin C, Jing W. Preliminary study on mouse interleukin 21 application in tumor gene therapy. Cell Mol Immunol. 2004;1: 461–6.
20. Matsui W, Huff CA, Wang Q. Characterization of clonogenic multiple myeloma Cells. Blood. 2004;103:2332–6.
21. Dou J, Pan M, Wen P. Isolation and identification of cancer stem like cells from murine melanoma cell lines. Cell Mol Immunol. 2007;4:528–33.
22. Hervé L, Michèle F, Sylvie G. A novel flow cytometric assay for quantitation and multiparametric characterization of cell-mediated cytotoxicity. J Immunol Methods. 2001; 253:177-87.
23. Naeem K, Donna B, Rachel B. T cell recognition patterns of immunodominant cytomegalovirus antigens in primary and persistent infection. J Immunol. 2007;178:4455–65.
24. Rosenberg SA, Sherry RM, Morton KE. Tumor progression can occur despite the induction of very high levels of self/tumor antigen-specific $CD8^{+}$T cells in patients with melanoma. J Immunol. 2005;175:6169–76.
25. Atanackovic D, Panse J, Hildebrandt Y. Surface molecule CD229 as a novel target for the diagnosis and treatment of multiple myeloma. Haematologica. 2011;96:1512–20.
26. Kim HS, Park HM, Park JS, Sohn HJ, Kim SG, Kim HJ, Oh ST, Kim TG. Dendritic cell vaccine in addition to FOLFIRI regimen

improve antitumor effects through the inhibition of immunosuppressive cells in murine colorectal cancer model. Vaccine. 2010;28:7787–96.
27. Kenichi A, Shin E, Ayumi Y. Targeting apoptotic tumor cells to FcγR provides efficient and versatile vaccination against tumors by dendritic cells. J Immunol. 2003;170:1641–8.
28. Ulrike B, Jörg SC, Ulrich W. A reciprocal repression between ZEB1 and members of the miR-200 family promotes EMT and invasion in cancer cells. EMBO Rep. 2008;9:582–9.
29. Su HY, Lai HC, Lin YW. Epigenetic silencing of SFRP5 is related to malignant phenotype and chemoresistance of ovarian cancer through Wnt signaling pathway. Int J Cancer. 2010;127:555–67.
30. Berx G, Raspe E, Christofori G. Pre-EMTing metastasis? Recapitulation of morphogenetic processes in cancer. Clin Exp Metastasis. 2007;24:587–97.
31. Robert S, Park SM, Andrea EM. mir-200c regulates induction of apoptosis through CD95 by targeting FAP-1. Mol Cell. 2010;38:908–15.
32. Mikesh LM, Kumar M, Erdag G. Evaluation of molecular markers of mesenchymal phenotype in melanoma. Melanoma Res. 2010;20:485–95.
33. Jun D, Ning G. Emerging strategies for the identification and targeting of cancer stem cells. Tumor Biol. 2010;31:243–53.
34. Bracken CP, Gregory PA, Kolesnikoff N. A double-negative feedback loop between ZEB1-SIP1 and the microRNA-200 family regulates epithelial-mesenchymal transition. Cancer Res. 2008;68:7846–54.
35. Ulrich W, Jörg SC, Ulrike CB, et al. The EMT-activator ZEB1 promotes tumorigenicity by repressing stemness-inhibiting microRNAs. Nat Cell Biol. 2009;12:1487–95.
36. Allen M, Jones JL. Jekyll and Hyde: the role of the microenvironment on the progression of cancer. J Pathol. 2011;223:162–76.